

## **DEVELOPMENT AND MODELING OF A NOVEL COMBINED WASHING AND THICKENING PROCESS**

Dipl.-Ing. J. Jeras, Dipl.-Math. techn. M. Feist,  
Dr.-Ing. H. Anlauf, Prof. Dr.-Ing. H. Nirschl\*  
Karlsruher Institut für Technologie (KIT), Institut für MVM, D-76131 Karlsruhe  
Tel:+49(0)721-608-42429; Fax:+49(0)721-608-42403

### **ABSTRACT**

Process machines are routinely used for the thickening of suspensions, where particles are separated in the gravitational field on basis of their specific weight. In these apparatuses, so called clarifier-thickener units, the principles of solid-liquid-separation are sedimentation and consolidation. In the chemical, and particularly in the pharmaceutical industry, the obtained thickened sludge from the underflow must often be washed in a second unit operation (e.g. filter cake washing or dilution washing) to remove dissolved impurities. The present industry-oriented research project in cooperation with Birken AG and Schrader GmbH & Co. KG is focused on the development and modeling of a new and innovative combined one-step washing and thickening process. Experimental results from a batch, laboratory-scale measurement setup and a continuous pilot washing-unit are shown and discussed.

### **KEYWORDS**

solid-liquid separation, sedimentation, washing, thickening

### **1. Introduction**

The here presented combined process step is primarily designed on a conical thickener. In the classic thickening procedure, suspensions enter the thickener while clarified liquid (overflow) and thickened sludge (underflow) leave the apparatus. The liquid concentration of unwanted, dissolved substances cannot be reduced. Therefore, in the novel process a fourth stream of pure, clear liquor is conducted in the bottom part of the thickener. By introduction of this fourth stream, particles can now settle from an impurity-laden layer into an impurity-free zone. The washing performance depends on the stratification quality of the environment. Hence it is mandatory to create a widely turbulence free flow inside the combined washer-thickener facility. Additionally, particle settling influences the success of washing: particles from the suspension inlet continuously settle across the stratified ambience. Figure 1-1 shows the principle of the process: A sharp density gradient inside the thickener is needed to prevent fluid convection. The pycnocline can be produced by simple temperature difference or, if the process allows, by adding salts in the lower layer or by adding specific lighter liquids to the upper layer (e.g. ethanol to water). For acceptable flow rate, experiments have shown that a temperature difference of one

degree can be high enough to create a stable density profile in the apparatus. Unwanted convection can be reduced by using a baffle plate to redirect the suspension inflow.

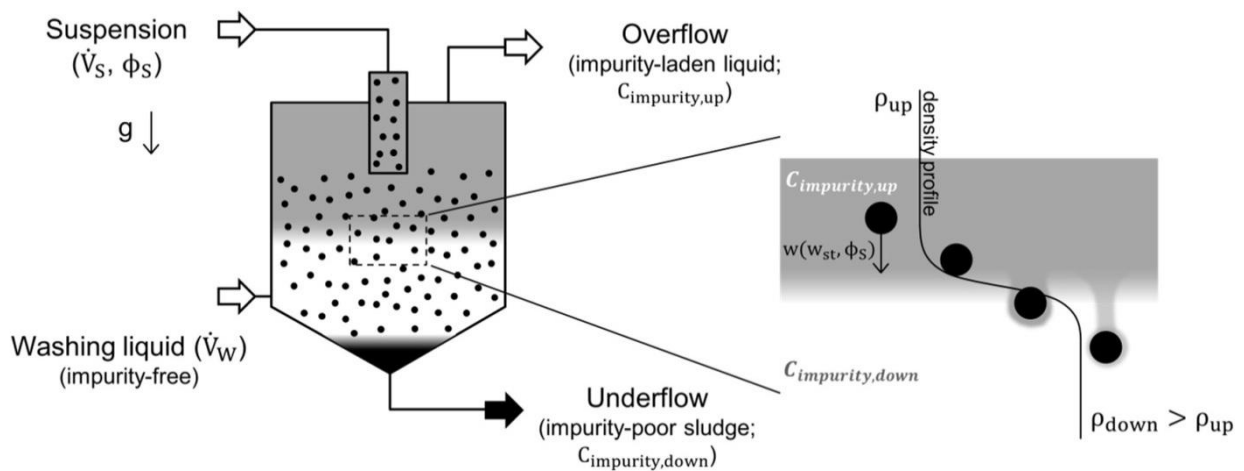


**Figure 1-1: Process principle.**

To estimate the liquid entrainment rate by settling particles, investigations for varying mass flow, particle size and density differences, have been done.

## 2. Materials and Methods

All experiments were conducted with water-based suspensions. Ethanol was added in varying concentrations to the upper layer to adjust the density difference. It is possible to exclude any surface tension effects, due to the total miscibility of water and ethanol. Consequently entrainment of impurity contaminated liquid is only influenced by the convection velocity and direction in the washer and by the settling particles themselves. While convection can be actively controlled by the suspension inflow rate, the apparatus geometry (e.g. installation of baffle plates) or with the density difference of the layers, the particle-induced entrainment depends to a high degree on product-related qualities such as particle size or form.

It was discovered that the so-called Richardson number plays a dominant role in describing experimental results. This dimensionless quantity represents the importance of natural convection relative to the forced convection:

$$\text{Ri} = \frac{\text{free convection}}{\text{forced convection}} = \frac{\text{Gr}}{\text{Re}^2} = \frac{g\Delta\rho L_c}{\rho w^2} = g' \frac{L_c}{w^2} \quad . \quad 2.1$$

It is utilized anywhere where buoyant forces are an important factor e.g. oceanography or meteorology. Fundamental principles are explained in detail in Turner [1].

## 2.1 Particles and fibers

In table 2-1 the particles and fibers are characterized. The main experiments were done with glass-beads.

**Table 2-1: Investigated particles and fibers.**

name	material	density	size	porosity
glass-beads*	SiO <sub>2</sub> , Na <sub>2</sub> O, CaO and others	2,5 g/cm <sup>3</sup>	Particle size fractions: 0-50; 40-70; 90-150; 100-200 µm	non-porous
PES-fibers**	polyethersulfon	1,4 g/cm <sup>3</sup>	Length: 1,6 mm Diameter: 0,14 mm	non-porous

\* SiLibeads Microbeads (glass-beads) supplied by Sigmund Lindner GmbH.

\*\* PES-fibers supplied by STW Schwarzwälder Textil Werke Heinrich Kautzmann GmbH.

## 2.2 Continuous pilot plant facility

Figure 2-1 (right) shows the used pilot plant facility. The facility was used for all investigations concerning convection optimization, layer stability and inflow-rate variation. A baffle plate was installed as depicted to redirect the suspension inflow in horizontal direction in order to preserve the liquid layer below. To visualize the layer position blue dye was used. The density difference was created by adding ethanol to the water-based suspension. The conical washer is 550 mm high and has a diameter of 443 mm in the broadest part. The volume content of the device is about 30 liters in all. The Inflow-rate of the suspension was varied from 37,5 l/h up to about 138,5 l/h.

## 2.3 Lab-scale batch measuring device

To quantify the entrainment-rate by the settling particles a lab-scale batch device was used (Figure 2-1, left). It consists of an ordinary measurement cylinder, with three integrated samplers (disposable syringes) to quantify the ethanol concentration in different heights. All experiments were conducted as follows: First of all water was added to a certain height and an blue colored ethanol-water mixture (figure 2-1, left) was added delicately on top. After that particles (or fibers) were added on the surface constantly with a defined mass-flow  $\dot{m}_p$ . After a defined amount of added particles  $\Delta m_p$  the procedure was stopped and the ethanol concentration along the cylinder height was measured (using an oscillating u-tube density meter by Anton Paar GmbH). As we could prove, the ethanol concentration in the lower layer is increasing with the amount of particles already settled, but is absolutely constant over the height. The entrainment-rate  $E_V$  can therefore be determined by the following equation:

$$E_V = \frac{V_{\text{entrained}}}{V_{\text{particles}}} = \frac{\Delta C_{V,\text{EtOH,down}} V_{\text{down}} \frac{1}{C_{V,\text{EtOH,up}}}}{\Delta m_p \frac{1}{\rho_p}} \quad 2.2$$

Finally, in order to obtain statistical certainty the procedure was repeated for at least two times. Additionally the method of supplying the particles was varied as shown in figure 2-2. Particles were homogenous scattered on the surface of the upper layer (a) or were supplied in presuspended form in the cylinder (b). Our investigations have shown that the entrainment-rate is independent of the method of particle distribution.

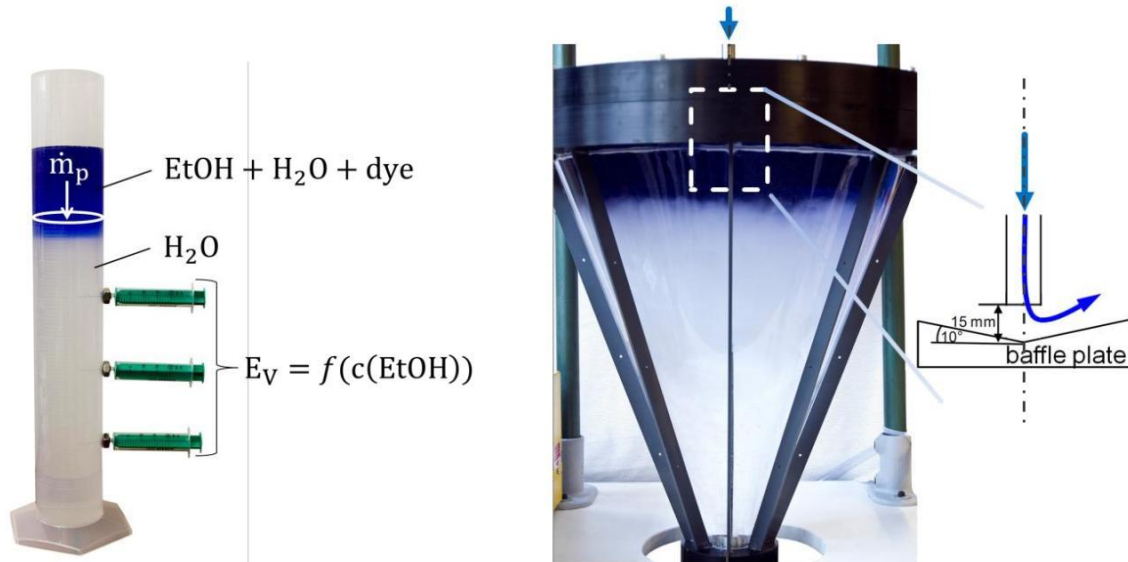


Figure 2-1: Lab-scale batch (left) and continuous pilot-plant (right) facilities.

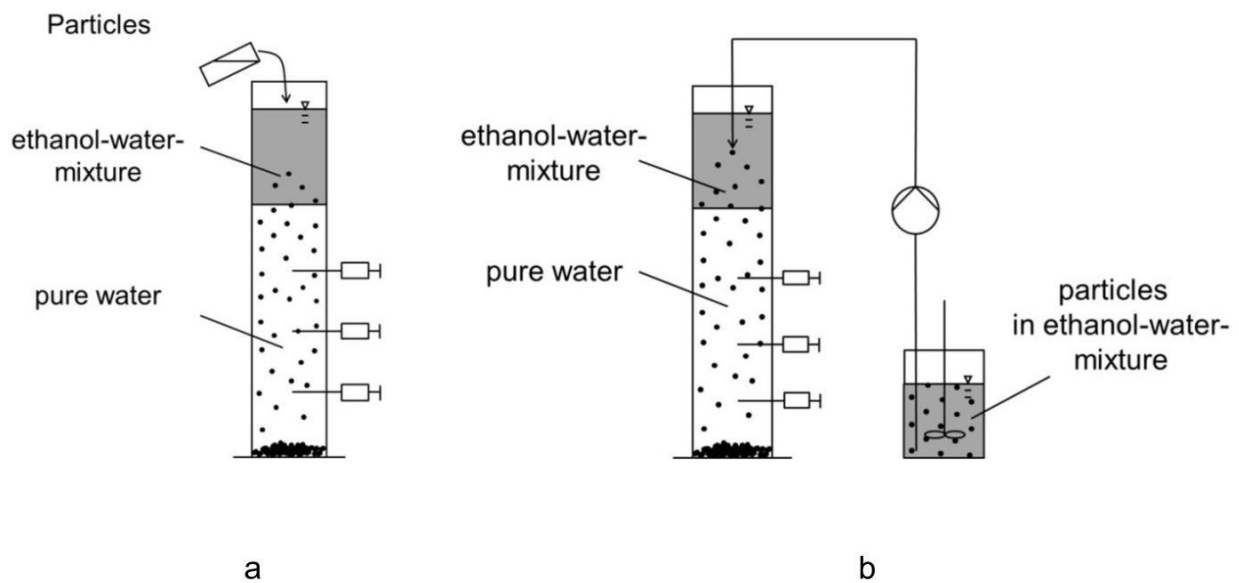


Figure 2-2: experimental setup: a. Particles are scattered on the surface; b. particles are presuspended.

### 3. Results

#### 3.1 Pycnocline stability and position

The continuous pilot-plant shown in figure 2-1 was used to investigate the density layer stability and position. The influencing parameters temperature difference and input flow rate had been varied. As the upper layer was dyed the pycnocline position could be detected visually. All layer positions were noted as heights  $\Delta X$  relative to the baffle plate (figure 3-1). The results are here presented as a function of the Richardson number:

$$Ri = \frac{L_c \Delta \rho}{w^2 \rho} g = \frac{d_{\text{inlet pipe}} \Delta \rho}{(w_{\text{inlet pipe}})^2 \rho_{\text{down}}} g \quad . \quad 3.1$$

$$d_{\text{inlet pipe}} = 0,012 \text{ m}$$

For temperature difference measurements (squares in figure 3-1) the temperature of the lower layer was hold constant by 18 °C ( $\rho_{\text{down}} = 998,57 \text{ kg/m}^3$ ) and the temperature of the upper layer was varied from 19 °C up to 26 °C ( $\rho_{\text{up}} = 998,40 - 996,78 \text{ kg/m}^3$ ). The input flow rate was hold constant by 138,5 l/h.

The water input flow rate was varied from 37,5 to 138,5 l/h (circles in figure 3-1), while the temperature difference stayed constant at  $\Delta T = 4 \text{ °C}$  ( $T_{\text{down}} = 18 \text{ °C}$ ;  $T_{\text{up}} = 22 \text{ °C}$ ).

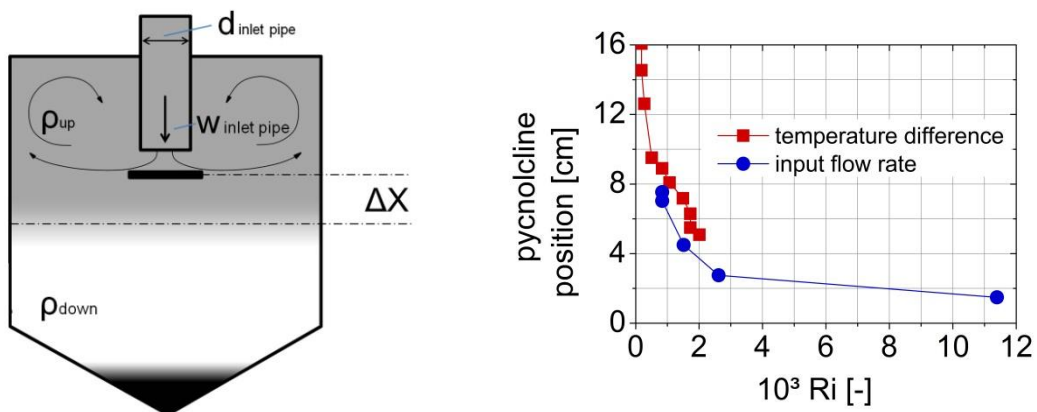


**Figure 3-1: Pycnocline position relative to the baffle plate ( $\Delta X$ ).**

Our investigations show that the layer stability is guaranteed within a wide range of values. The installed baffle plate deflects the input flow and prevents from unwanted convections vertical to the layer. A temperature difference of  $\Delta T = 4 \text{ °C}$  generates enough buoyancy to oppose inflow-forced convection up to high input rates (138,5 l/h). For temperature differences of less than  $\Delta T = 1 \text{ °C}$  convective forces dominate and no stable density-layer was observed.

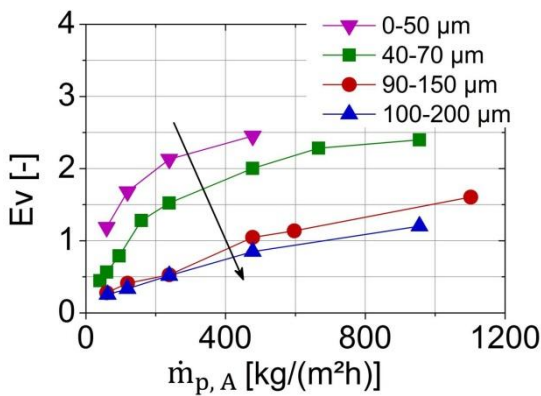
### 3.2 Entrainment rate and settling particles

Particles continuously transport impurity laden liquid across the pycnocline. Lab scale batch measurements were conducted as presented in section 2.3. The area specific mass-flow-rate  $\dot{m}_{p,A}$ , the particle size and the density differences of the liquid layer had been varied (figure 3-2 a-c).

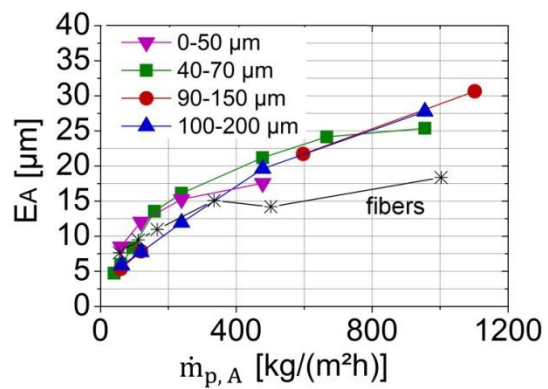
All results show that the entrainment-rate  $E_V$  is increasing with the area specific mass-flow rate. The investigations on influence of particle size are presented in figure 3-2 a. Apparently the entrainment-rate is decreasing with increasing particle size. In figure 3-2 b results of particle size variation are plotted over the area specific entrainment-rate which is defined as follows:

$$E_A = E_V \frac{V_{\text{particles}}}{A_{\text{particles}}} = \frac{V_{\text{entrained}}}{A_{\text{particles}}} \quad 3.2$$

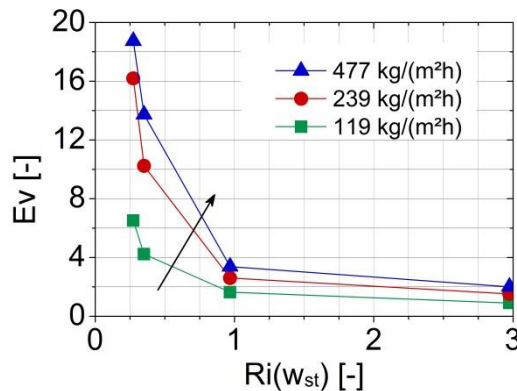
As depicted, all curves of the particle size variation (figure 3-2 a) form one master curve (figure 3-2 b).



(a) particle size variation (glass-beads).



(b) particle size variation (glass-beads) and PES-fibers.



(c) buoyant force variation for glass-beads (40-70 μm).

**Figure 3-2: Entrainment due to settling particles: Variation of particle size, buoyant force and mass flow.**

Comparative measurements with PES-fibers (very low  $V_{\text{particles}}/A_{\text{particles}}$ -ratio) were done. Until an area specific mass-flow-rate of about 300 kg/(m<sup>2</sup>h) the curve of PES-fibers lies on the master curve of the glass-beads. For higher mass flow it bottoms out much faster as the master curve. It must be assumed that the fibers reach their critical flux for around 300 kg/(m<sup>2</sup>h). The critical flux is reached when suspension is faster supplied as particles can settle down. From that point on particles are transported in a great measure to the overflow of a classic thickener.

Entrainment rates assigned in figure 3-2 a and b were measured with density differences of  $\Delta\rho = \rho_{\text{down}} - \rho_{\text{up}} = \rho_{\text{Water, 20}^\circ\text{C}} - \rho_{\text{Ethanol, 20}^\circ\text{C}} \approx 208 \text{ kg/m}^3$ . The influence of buoyancy are presented in diagram c. Here the Richardson number was calculated as follows:

$$\text{Ri}(w_{\text{st}}) = \frac{L_c \Delta\rho}{w^2 \rho} g = \frac{x_{50} \Delta\rho}{(w_{\text{st}, x_{50}} (\text{water, 20}^\circ\text{C}))^2 \rho_{\text{down}}} g \quad . \quad 3.3$$

The Ethanol volume concentration in the upper layer was varied from  $C_{V, \text{EtOH}, \text{up}} = 100\%$  down to 15% ( $\Delta\rho \approx 208$  down to  $19 \text{ kg/m}^3$ ). The curves in figure 3-2 c show, that the entrainment-rate is dramatically increasing for small density differences. While layer stability was possible for temperature differences of less than  $\Delta T = 4 \text{ }^\circ\text{C}$  ( $\Delta\rho < 1 \text{ kg/m}^3$ ) (section 3.1), the entrainment-rate seems to be the constraining factor of the process. For density differences of  $19 \text{ kg/m}^3$  water temperature differences of more than  $40 \text{ }^\circ\text{C}$  would be necessary.

#### 4. Conclusions

The presented investigations show the potential of the new process. Further investigations have to be done.

#### Acknowledgements

The authors would like to thank the AIF (Allianz Industrie Forschung) for their financial support. We also wish to acknowledge our Project partners from Birken AG and Schrader GmbH & Co. KG for their support and assistance.

## Nomenclature

Symbol	Definition	Unit
$C_{\text{impurity,down}}$	impurity concentration in the lower layer	mol/l
$C_{\text{impurity,up}}$	impurity concentration in the upper layer	mol/l
$C_{V,\text{EtOH,down}}$	ethanol concentration in the lower layer	$\text{m}^3/\text{m}^3$
$C_{V,\text{EtOH,up}}$	ethanol concentration in the upper layer	$\text{m}^3/\text{m}^3$
$E_V$	entrainment (-rate)	-
$E_A$	area specific entrainment (-rate)	$\mu\text{m}$
$g$	gravity	$\text{m}/\text{s}^2$
$g'$	reduced-gravity	$\text{m}/\text{s}^2$
$Gr$	Grashof number	-
$L_c$	characteristic length	m
$\dot{m}_p$	mass-flow of particles	kg/h
$\dot{m}_{p,A}$	area specific mass-flow rate of particles	$\text{kg}/(\text{m}^2\text{h})$
$m_p$	mass of particles	kg
$Ri$	Richardson number	-
$Re$	Reynolds number	-
$V_{\text{down}}$	volume of the lower layer	$\text{m}^3$
$w$	velocity	$\text{m}/\text{s}$
$w_{\text{st}}$	stokes particle settling velocity	$\text{m}/\text{s}$
$w_{\text{inlet pipe}}$	fluid flow velocity in the inlet pipe	$\text{m}/\text{s}$
$x_{50}$	median particle size	$\mu\text{m}$
$\rho$	density	$\text{kg}/\text{m}^3$
$\phi$	solid volume concentration	$\text{m}^3/\text{m}^3$

## References

[1] Turner, J. S. (1973), Buoyancy effects in fluids, Cambridge Univ. Press, 313 et seq.